

Microscopic investigation of single-wall carbon nanotube uptake by Daphnia magna

The Faculty of Oregon State University has made this article openly available.
Please share how this access benefits you. Your story matters.

Citation	Edgington, A. J., Petersen, E. J., Herzing, A. A., Podila, R., Rao, A., & Klaine, S. J. (2014). Microscopic investigation of single-wall carbon nanotube uptake by Daphnia magna. <i>Nanotoxicology</i> , 8, 2-10. doi:10.3109/17435390.2013.847504
DOI	10.3109/17435390.2013.847504
Publisher	Informa Healthcare
Version	Version of Record
Terms of Use	http://cdss.library.oregonstate.edu/sa-termsfuse

ORIGINAL ARTICLE

Microscopic investigation of single-wall carbon nanotube uptake by *Daphnia magna*

Aaron James Edgington¹, Elijah J. Petersen², Andrew A. Herzing², Ramakrishna Podila³, Apparao Rao³, and Stephen J. Klaine¹

¹Institute of Environmental Toxicology, Clemson University, Pendleton, SC, USA, ²Material Measurement Laboratory, NIST, Gaithersburg, MD, USA, and ³Department of Physics and Astronomy, Clemson University, Clemson, SC, USA

Abstract

The objectives of this study were to determine the extent of absorption of functionalized single-wall carbon nanotubes (SWCNTs) across the gut epithelial cells in *Daphnia magna*. Several microscopic techniques were utilized, including micro-Raman spectroscopy, high-resolution transmission electron microscopy (HRTEM) and selective area diffraction (SAD). In an effort to examine the variation in uptake due to surface properties, four groups of differently functionalized SWCNTs were used: hydroxylated (OH-SWCNTs), silicon dioxide (SiO₂-SWCNTs), poly aminobenzenesulfonic acid (PABS-SWCNTs) and polyethylene glycol (PEG-SWCNTs). Raman spectroscopy was able to detect OH-SWCNTs within the gut, but lacked the spatial resolution that is needed to identify lower concentrations of SWCNTs that may have been absorbed by body tissues. Initially, low-magnification imaging of exposed *D. magna* sections in the TEM revealed several features, which suggested absorption of SWCNTs. However, subsequent analysis with additional techniques (HRTEM, X-ray energy-dispersive spectroscopy and SAD) indicated that these features were either artifacts produced via the specimen staining process or consisted of non-graphitic, organic structures. This latter observation emphasizes the inherent difficulty in resolving SWCNTs embedded within a complex, organic matrix, as well as the care with which imaging results must be interpreted and supplemented with other, more analytical techniques.

Keywords

Absorption, electron microscopy, nanomaterials

History

Received 24 September 2012

Revised 14 July 2013

Accepted 18 September 2013

Published online 18 December 2013

Introduction

Single-wall carbon nanotubes (SWCNTs) are an allotrope of carbon characterized by strong covalent bonding between carbon atoms, a high aspect ratio, high tensile strength and high electron conductance (Iijima, 1991; Niyogi et al., 2002). These characteristics have made SWCNTs useful for a variety of applications within the electronics, computer and aerospace industries (Lam et al., 2004). As the demand for products containing nanomaterials increases, the scale of nanomaterial manufacturing will grow, with current calculations predicting an annual carbon nanotube (CNT) production of over 18 000 kg (20 t) in USA (Gottschalk et al., 2009). A likely consequence of increased production is an increase in the future environmental release of manufactured nanomaterials (Maynard et al., 2006), which will ultimately result in their entry into aquatic ecosystems.

There are many naturally occurring colloids that exist in aquatic ecosystems that have the potential to adsorb to carbon nanomaterials and influence their aqueous stability; consequently impacting their fate and bioavailability to aquatic organisms. One such colloid is natural organic matter (NOM), a complex heterogeneous molecule that is ubiquitous in all surface waters. It varies in both molecular weight and chemical composition having both hydrophilic and lipophilic components (Gottschalk

et al., 2009). Researchers have shown that NOM can adsorb onto the surface of carbon nanotubes and influence their aqueous stability, which will lead to changes in environmental transport (Edgington et al., 2010; Hyung et al., 2007; Hyung & Kim, 2008; Lu & Su, 2007; Zhang et al., 2011). It has also been shown that water quality characteristics, such as pH and ionic strength, affect the stability of NOM/nanomaterial suspensions (Hyung et al., 2007). Further, it has been suggested that the various properties of the NOM source may have an effect on nanomaterial stability and toxicity (Chappell et al., 2009; Gottschalk et al., 2009). Finally, proteins are another naturally occurring organic component found in aquatic ecosystems, and researchers have shown that they frequently bind to the surface of nanomaterials. The resulting protein corona significantly increases the bioavailability of the underlying nanomaterials (Cedervall et al., 2007; Lundqvist et al., 2008).

In vitro studies have shown that SWCNTs can cause a number of adverse effects in a variety of cell lines (Cheng et al., 2011; Davoren et al., 2007; Di Giorgio et al., 2011; Wang et al., 2011). However, few, if any, of these have been confirmed with *in vivo* studies. Inhalation studies with mice have shown that SWCNTs can cause inflammation responses and gross morphological abnormalities in lung tissues (Inoue et al., 2010; Lam et al., 2004). Templeton et al. (2006) found reduced survival rates for the estuarine meiobenthic crustacean copepod *Amphiascus tenuiremis* in concentrations ranging from 0.97 to 10 mg/L SWCNTs, with the 10 mg/L treatment producing reduced life stage development. Smith et al. (2007) reported an increased

incidence of oedema and enlarged mucocytes in exposed rainbow trout gills, but a more recent study by Fraser and coworkers did not find toxic effects in fish that were fed SWCNT-spiked food at a concentration of 500 mg/kg of food (Fraser et al., 2011). Additionally, high concentrations of SWCNTs have generally not caused substantial toxic effects in sediment and soil organisms (Ferguson et al., 2008; Galloway et al., 2010; Petersen et al., 2008a,b, 2009). For example, while evidence of the passage of CNTs through the gut of organisms such as earthworms and oligochaetes has been observed, evidence of their bioaccumulation has not been determined (Ferguson et al., 2008; Galloway et al., 2010; Petersen et al., 2008a,b, 2010). A similar finding was observed in a recent study assessing SWCNT bioaccumulation and trophic transfer using near infrared fluorescence (NIRF) which did not indicate bioaccumulation in the amphipod *Ampelisca abdita* and the mysid *Americamysis bahia* (Parks et al., 2013). However, these studies have generally not used advanced imaging techniques such as electron microscopy to investigate CNT absorption into the organism tissues, and thus absorption of small SWCNT masses could not be excluded when the SWCNT concentration in the whole organism was quantified. In one study that did investigate SWCNT uptake in lugworms (*Arenicola marina*) using transmission electron microscopy (TEM) and coherent anti-stokes Raman scattering microscopy (CARS), absorption of SWCNTs from sediments into the organisms was not observed (Galloway et al., 2010). Furthermore, knowledge regarding the absorption and accumulation of SWCNTs in whole organism models exposed to lower concentrations in environmentally relevant conditions is lacking.

The objectives of this research were to determine the absorption of SWCNTs across the gut tract of *Daphnia magna* and to determine if absorption was influenced by SWCNT surface functionalization. In the process of conducting this research, we also investigated the suitability of various characterization techniques for confirming the biological uptake behavior of SWCNTs.

Materials and methods

Organisms

Daphnia magna were obtained from cultures maintained at the Institute of Environmental Toxicology, Clemson University (Pendleton, SC). They were cultured in U.S. Environmental Protection Agency (U.S. EPA) moderately hard reconstituted water (MHW) at 25 °C with a 16:8 h light:dark cycle (Lewis et al., 1994; U.S. Environmental Protection Agency, 1993).

SWCNTs

Four different functionalized SWCNTs were used in this study. Hydroxylated SWCNTs (OH-SWCNTs) were purchased from cheaptubes.com (Brattleboro, VT). A sample of this material was then further functionalized by Dr. Mukhopadhyay's laboratory at Wright State University (Dayton, OH) with silicon dioxide (SiO₂-SWCNTs). Poly aminobenzenesulfonic acid (PABS-SWCNTs) and polyethylene glycol (PEG-SWCNTs) functionalized SWCNTs were purchased from Carbon Solutions, Inc (Riverside, CA). These functional groups were chosen because of their differences in polarity and size. Transmission electron micrographs of the SWCNTs were taken after sonication to determine material length and diameter.

Natural organic matter

The NOM source used during this study was Suwannee River NOM (SR-NOM) that was concentrated to a powder by reverse osmosis (lot # 1R101N, International Humic Substances Society).

Natural organic matter solutions were made by diluting SR-NOM in moderately hard water (MHW) and then filtering it with a 0.2- μ m cellulose membrane filter prior to toxicity tests. All tests and dilution water were used at concentrations of \sim 2.5 mg/L dissolved organic carbon (DOC).

Hyclone standard fetal bovine serum (FBS) (Logan, UT) was the protein source and was used as received.

SWCNT suspensions

Single-wall carbon nanotubes were suspended in SR-NOM solution using the following procedure. The SWCNT sample was first weighed on aluminum foil and placed in a 100-mL glass centrifuge tube to which 100 mL of SR-NOM solution was then added. This suspension was then probe sonicated with a Branson digital sonifier (Danbury, CT) for 20 min at 40% power. The power output in this interval was calculated to be \sim 85.2 W using the method described by (Taurozzi et al., 2010). Dispersions were then allowed to settle for \sim 24 h before the supernatant was used for bioassays. Concentrations of SWCNTs in suspension were determined gravimetrically by weighing the remaining tubes after withdrawal of the supernatant (see below).

Hydroxylated SWCNTs were suspended with FBS using the following procedure: the material was first weighed on aluminum foil and placed in a glass centrifuge tube; 8 mL of FBS solution was added to the centrifuge tube, and the solution was bath sonicated (Fisher Scientific model FS30) for 10 min (\sim 100 W). The SWCNT-FBS solution was diluted to 100 mL with MHW and then probe sonicated for an additional 10 min. The protein concentration for this solution was \sim 2.5 mg/L. The solutions were allowed to settle for \sim 24 h before the supernatant was used for bioassays.

The stable solution was decanted and concentrations were determined by weighing the remaining precipitate on a pre-rinsed 0.2 μ m cellulose membrane filter after the filter had dried. This mass was subtracted from the initial mass of SWCNTs and divided by the volume of the stable stock solution to determine the initial stock concentration. The stock solution was further diluted with NOM solution to achieve a SWCNT concentration of 1 mg/L for bioassays.

Particle characterization

To determine particle size, all materials used in exposures were imaged after sonication in NOM solutions. Single drops of stock solutions were allowed to dry on 200 mesh copper TEM grids (Electron Microscopy Science, Hatfield, PA). Images were taken on a Hitachi 7600 TEM at 120 kV. Particle size was determined qualitatively through examination of the imaged material and quantitatively using Image J software for point-to-point measurements of the dried SWCNT suspensions. Electrophoretic mobility (EM) in the stock solution was determined using a Malvern Zetasizer (Malvern Instruments, Worcestershire, UK). Solution conductivity and pH were also recorded.

Bioassays

Daphnia magna acute 96 h static renewal bioassays were performed following U.S. EPA methods (Lewis et al., 1994; U.S. Environmental Protection Agency, 1993) with the exception that only one concentration (1 mg/L) and three replicates were used for each SWCNT. In addition, a NOM control was also used with three replicates. Briefly, 15 mL of either SWCNT or control solution was added to each 30 mL glass beaker test chambers. Five organisms, <24 h old, were placed in each test chamber. Test solutions were renewed daily and fed 0.25 mL of a 4:3 ratio

of algae and yeast/trout chow/cereal (YTC) 2–4 h before renewal. The 1 mg/L SWCNT dose was chosen because preliminary data showed it to cause no acute toxicity (mortality) yet allowed for a visibly full gut when examined by the naked eye.

Micro-Raman spectroscopy sample preparation and analysis

After 96 h, active *D. magna* were fixed in 4% glutaraldehyde solution overnight and, after dehydration steps with ethanol solutions, embedded in Immunobed resin and sectioned on a microtome to $\sim 8 \mu\text{m}$ thick. Lateral sections of the whole organism were placed on glass slides for Raman spectroscopy analysis. The micro-Raman spectra were excited with a 514.5-nm laser line, and the laser power was maintained $\sim 1 \text{ mW}$ to avoid sample heating. A Leica microscope equipped with a $5\times$ dry objective was used to focus the laser beam, and the Raman scattered light was collected using an ISA Triax 550 spectrometer equipped with a liquid-nitrogen cooled CCD. A Kaiser Optics holographic notch filter was used for the rejection of Rayleigh scattered light from the sample.

Transmission electron microscopy sample preparation and analysis

After 96 h, active *D. magna* were fixed in 4% glutaraldehyde solution overnight and, after dehydration steps with ethanol solutions, embedded in LR White resin. The samples were polymerized at 90°C overnight then sectioned on an ultramicrotome. Sections of the organisms' midguts were placed on 200 mesh copper grids that had alphabetical coordinates for location purposes (Electron Microscopy Science, Hatfield, PA).

Preliminary imaging at low-magnification was carried out using a Hitachi 7600 TEM operating at 120 kV. Those samples where SWCNT absorption within *D. magna* was indicated using low-magnification TEM were then more fully analyzed using high-resolution transmission electron microscopy (HRTEM), selective area diffraction (SAD) and electron energy-loss spectroscopy (EELS) analyses in order to confirm particle identity. This data was acquired using an FEI Titan 80–300 TEM/STEM operating at 300 kV, which was equipped with a Gatan Tridiem 865 imaging energy-filter for EELS based analysis. HRTEM imaging was conducted in an effort to identify SWCNTs, because their presence should be conclusively identified via their amplitude and phase contrast relative to the surrounding amorphous organic matrix. In addition, when MWCNTs or a bundle of SWCNTs is encountered by the electron beam, the underlying crystallinity produces a distinct SAD pattern due to Bragg diffraction, whereas the pattern from the amorphous organic matrix will consist only of diffuse rings due to the lack of medium- and long-range order.

Results

Particle characterization

There were no significant differences observed between the electrophoretic mobilities measured from the CNT suspensions, with all solutions exhibiting a value of $\sim -1.5 \mu\text{m cm/Vs}$. There were also no significant differences in solution conductivity and pH. TEM micrographs indicated that the SWCNT lengths fell in a range between 0.75 and $2 \mu\text{m}$ while their diameter was $\sim 2 \text{ nm}$ for all materials tested (Figure 1).

Bioassays

There was no observed mortality in any of the controls or SWCNT treatments over the 96-h exposure period.

Raman spectroscopy

Samples of raw OH-SWCNTs were analyzed with Raman spectroscopy to determine the material's G and D band signal. The areas within the gut lateral section that had the same G and D band signal as the raw OH-SWCNTs were mapped (Figure 2). The mapped section shows a strong G and D band within the gut, and no signal within the tissues of the *D. magna*. This suggests that the gut is impacted with SWCNTs, as expected, but that the material is non-detectable within the other tissues. This method was repeated on another area of the section lower in the gut and with higher magnification. The resulting G-band signal is mapped and shows a highlighted region of high OH-SWCNT concentration within the gut region, but there is no signal outside of the gut region, indicating that SWCNTs absorption by other tissues was not detectable using Raman spectroscopy under these conditions (Figure 3).

Transmission electron microscopy

The TEM images of the sonicated SWCNTs suggest that the sonication creates a dispersed material without altering the structure of the SWCNTs (Figure 1). Although sonication of the PABS and PEG-SWCNTs in NOM (Figure 1C and D, respectively) resulted in dispersal into individual SWCNTs, sonication of OH- and SiO_2 -SWCNTs in NOM (Figure 1A and B) or OH-SWCNTs in FBS (Figure 1E) resulted in nanotube bundles. This more complete dispersion is likely due to the more favorable interaction between the hydrophilic PABS and PEG functional groups and the water molecules. However, it is possible that aggregation could have occurred for the OH-SWCNTs and the SiO_2 -SWCNTs as the solutions dried after drop casting onto the TEM grids.

Images acquired from the cross sections of the *D. magna* exposed to NOM dispersed OH-SWCNTs exhibited regions of dark contrast within the gut, on the microvilli, and embedded within the lumen (Figure 4A and B). While the size of these regions was far too large for them to be due to individual SWCNTs, they could represent larger aggregates of SWCNTs (Figure 4A and B). Similar regions were again seen in the cross sections of *D. magna* exposed to NOM dispersed PEG-SWCNT (Figure 4C and D). This material appeared to be more fiber-like, and was embedded well within the lumen (Figure 4C and D compared to Figure 4A and B). Other regions were observed that suggested SWCNT absorption, as seen in Figure 4E and F. A long tube shaped structure with dimensions comparable to a SWCNT bundle is embedded within the boundary layer between the microvilli and the lumen of the specimen exposed to NOM dispersed PABS-SWCNT (Figure 4F). No such regions were present in the *D. magna* exposed to NOM dispersed SiO_2 -SWCNTs (Figure 4G).

The images of the cross sections of the *D. magna* exposed to FBS dispersed OH-SWCNTs showed similar incidences of dark contrast associated with the microvilli and embedded within the lumen (Figure 4H and I). Figure 4I suggests that the material has a dark core with a lighter coating, which could be due to a protein corona surrounding the high electron density regions of the OH-SWCNT aggregates, as described earlier.

HRTEM, X-ray energy dispersive spectroscopy, SAD and Electron Energy- EELS

To further investigate the regions where uptake seemed to have occurred in FBS-coated OH-SWNTs, PABS-SWNTs and PEG-SWNTs according to low magnification TEM, HR-TEM, SAD and Energy Dispersive Spectroscopy (EDS) were utilized. The *D. magna* exposed to FBS-coated OH-SWCNTs samples

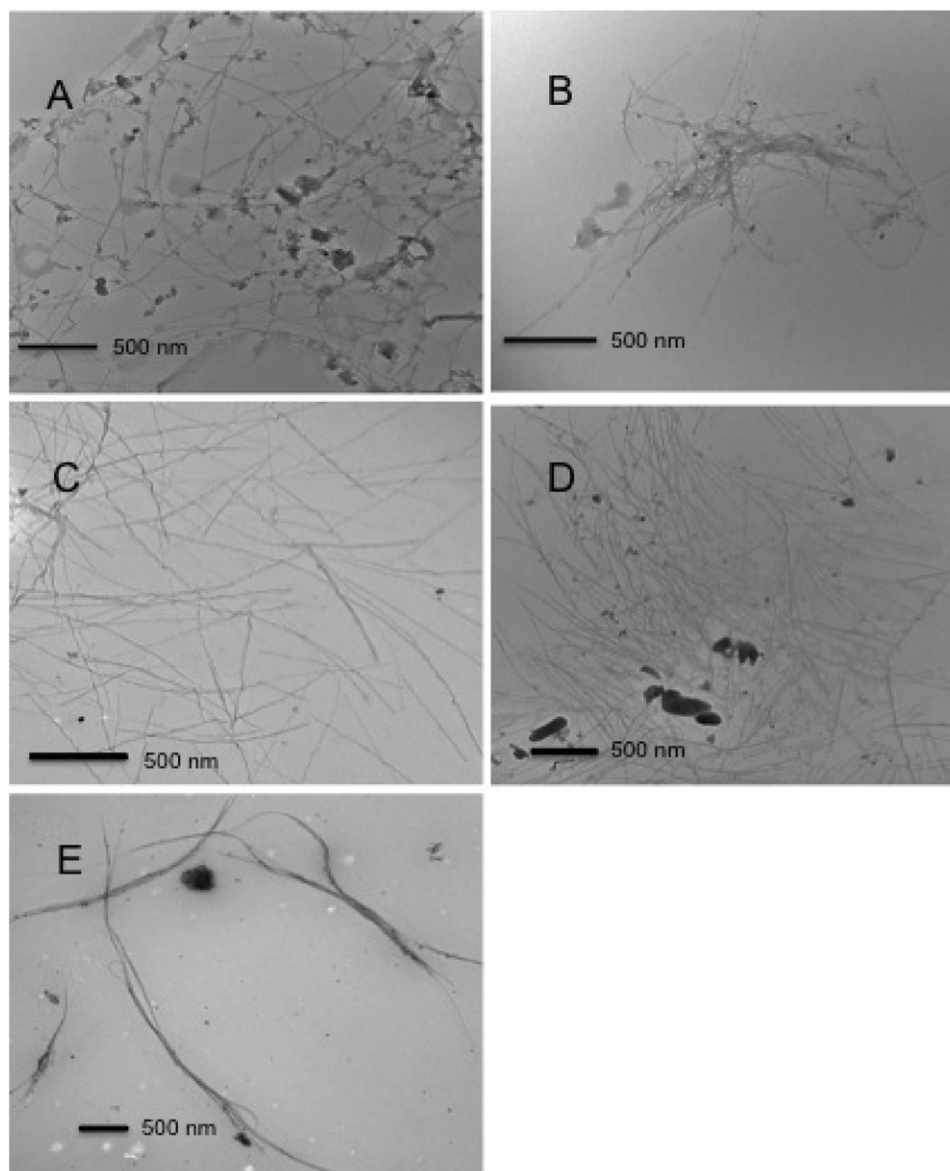


Figure 1. TEM images of materials post-sonication. (A) OH-SWCNTs in natural organic matter, (B) SiO₂-SWCNTs in natural organic matter, (C) PABS-SWCNTs in natural organic matter, (D) PEG-SWCNTs in natural organic matter and (E) OH-SWCNTs in FBS.

were further investigated to identify the dark and tube-like material found previously. Surprisingly, we were unable to find SWCNTs in the gut tracts or in the organism's tissues of these samples. In Figure 5A, the same tubular structures seen previously at low magnification were located, but when they were viewed at higher magnifications (Figure 5C), no SWCNTs were observed. Further, diffraction analyses of these regions suggested that the material was in fact amorphous, rather than exhibiting strong features due to Bragg diffraction (Figure 5C inset). For stained samples of the FBS OH-SWCNT exposed *D. magna* (Figure 4H and I), a large number of strongly-scattering particles was observed. Using EDS (data not shown), we determined that these particles contained mostly uranium and lead, indicating that they were a by-product of the staining process.

Electron energy-loss spectroscopy has been utilized to characterize and identify CNTs in previous studies (Egerton, 2009; Reed & Sarikaya, 2002), but in this study, EELS analysis proved to be inconclusive. While a strong EELS signal was produced by the sonicated SWCNTs directly added to the grids, it was substantially more challenging to use this technique to identify SWCNTs within the epoxy resins of the microtomed sections due

to the large background signal from the resin itself and the low concentration of SWCNTs present.

We also searched for SWCNTs in the gut tract of daphnia treated with PABS-SWCNTs (Figure 5D–F). We were able to find SWCNTs in numerous locations within the gut, clearly image the material at high magnification (Figure 5F), and confirm the results using SAD analysis. However, using electron diffraction to scan the tissues of the organisms to identify locations with SWCNTs proved to be unsuccessful. We also utilized HRTEM to investigate several locations, which were previously found to contain tubular structures at lower magnification, but did not locate nanotubes based on the phase-contrast exhibited by the HRTEM images or the features observed in the SAD patterns. Similar results were found in tissues from PEG-SWCNT exposed organisms (Figure 5G–I), where the areas of suspected SWCNT uptake were determined to be amorphous carbon using HR-TEM and SAD (Figure 5I).

Discussion

Several studies have been conducted to investigate carbon nanotube uptake by organisms using microscopic methods.

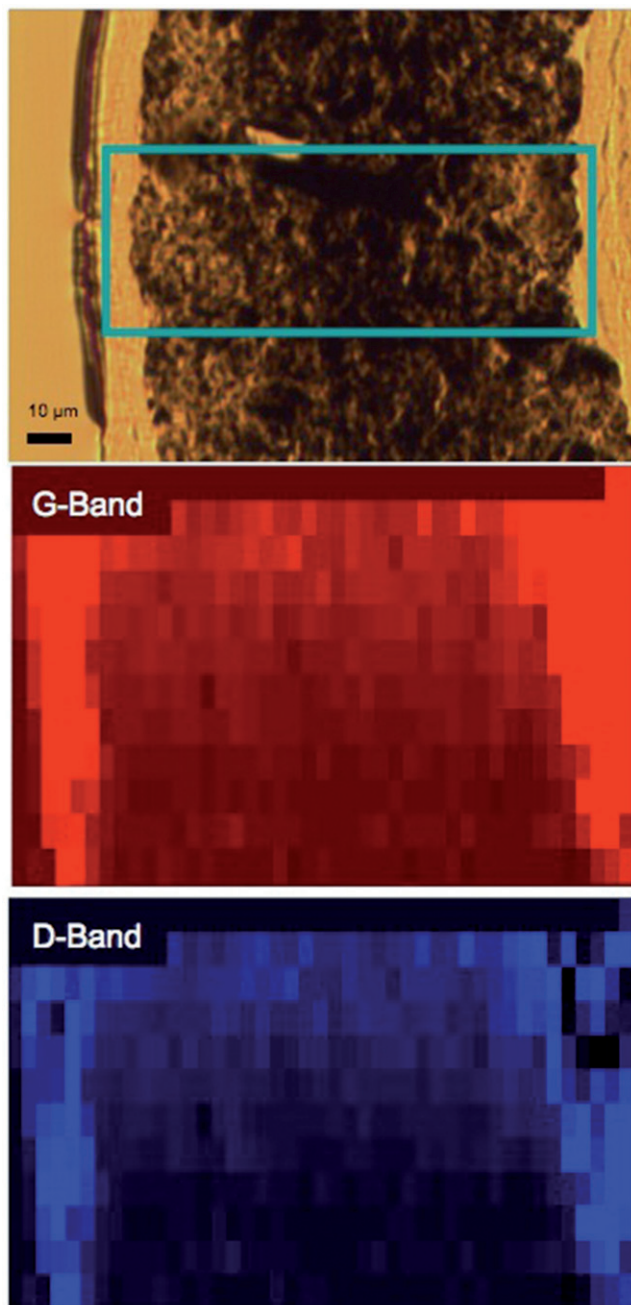


Figure 2. The top image is the sample to be analyzed; the left hand side is the dorsal surface of the sectioned *Daphnia magna* the blue square is the area analyzed by Raman Spectroscopy. The G-band and D-band signals are strong in the gut and absent at the edges indicating a high concentration of ingested OH-SWCNTs within the gut but no detectable signal in the tissues.

Roberts et al. (Roberts et al., 2007) characterized the behavior of lipid coated SWCNTs during exposure to *D. magna*. Using Raman spectroscopy and confocal fluorescent microscopy they were able to determine that the SWCNTs had completely impacted the gut, but they were unable to determine absorption from the gut to other tissues. Mouchet and coworkers (Mouchet et al., 2008, 2010) conducted several studies of the effects of CNT exposure on an amphibious model, the African clawed frog *Xenopus laevis*. After exposure to double-walled nanotubes (DWCNTs) or multi-walled carbon nanotubes (MWCNTs) for 12 days, they used light microscopy, TEM and Raman spectrometry to locate DWCNTs within exposed larvae. They observed dark masses within the intestinal tissues of exposed organisms using light microscopy and confirmed with Raman spectroscopy

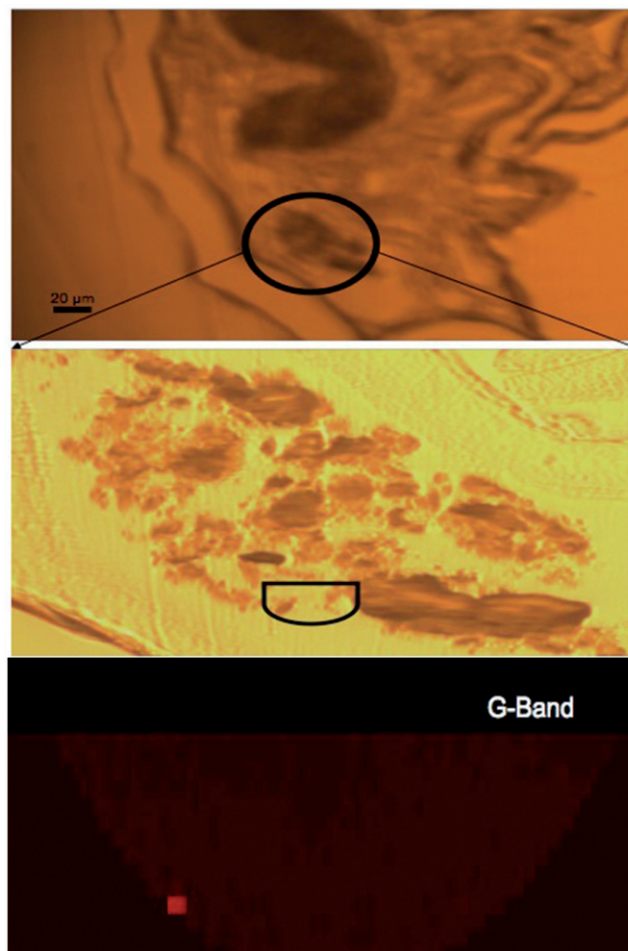


Figure 3. The top image is area of the gut chosen for analysis and in the second image the area analyzed at higher magnification is highlighted in black. The resulting G-band signal is mapped out and shows a highlighted region of high OH-SWCNT concentration within the gut of exposed *D. magna*, but there is no detectable signal within the tissues.

and HRTEM that within the dark masses, DWCNTs and MWCNTs were present. Furthermore, with HRTEM they were able to image what appeared to be DWCNTs and MWCNTs embedded within the lumen tissue. However, Raman spectroscopy analysis and HRTEM images suggest the material is unable to absorb across cell membranes. Edgington et al. (2010) characterized multi-walled carbon nanotubes (MWCNTs) once they were ingested by *D. magna* by imaging the midgut of sectioned organisms with TEM. MWCNTs were clearly seen within the gut and up against the microvilli layer, but were not seen within the lumen or other tissues. It was hypothesized that their diameter and length hindered their absorption across the cellular membranes of the lumen.

From the above studies, it is clear that useful methods for probing the absorption behavior of SWCNTs in an *in vivo* model are Raman spectroscopy and TEM. In the present study, Raman spectroscopy was able to detect OH-SWCNTs within the gut. However, due to the relatively large size of the laser diameter (5 μm) compared to the fine structures of the *D. magna* gut tract, the technique is not capable of locating the much lower concentrations of SWCNTs that may be absorbing into body tissues.

Therefore, we sectioned OH-SWCNT, SiO₂-SWCNT, PABS-SWCNT and PEG-SWCNT exposed *D. magna* in order to analyze them via TEM. Although low magnification TEM images suggested that there were several areas within the tissues where

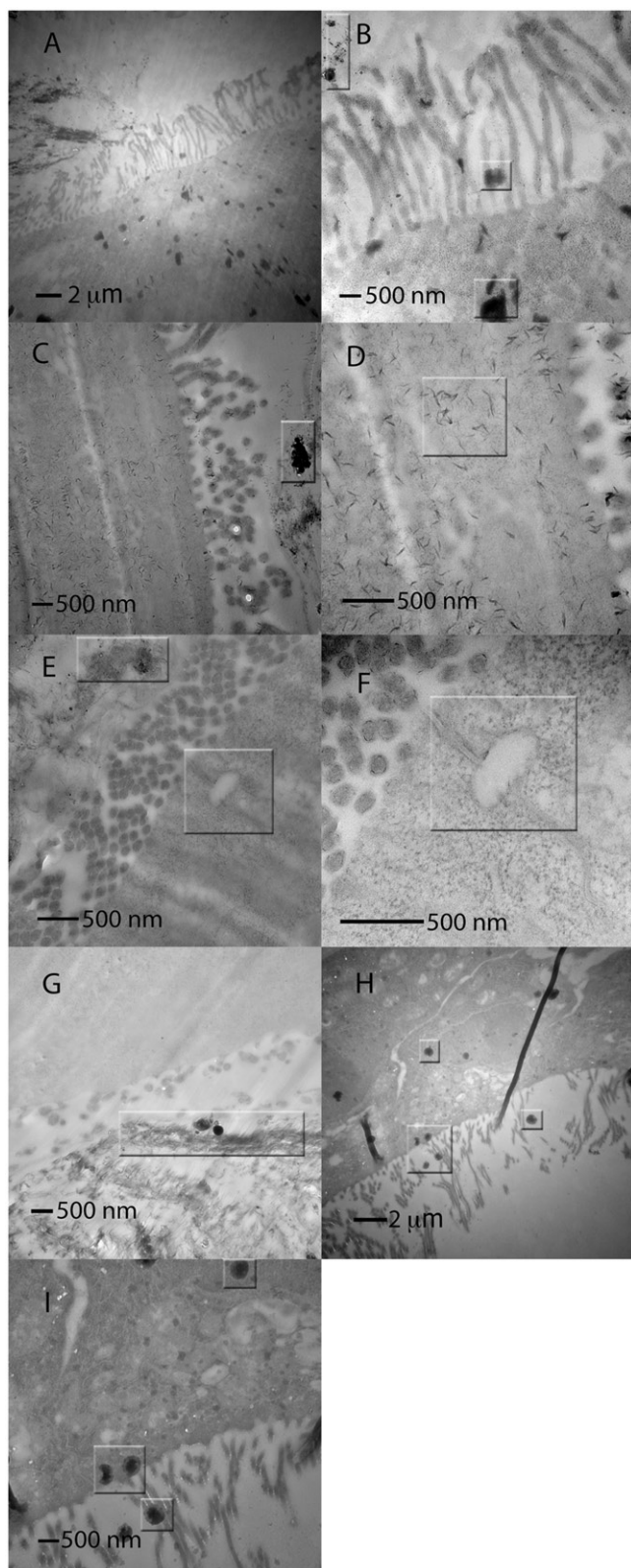


Figure 4. Transmission electron microscopy images of the cross section of suspended SWCNT-exposed *D. magna*. Images show the gut, microvilli and lumen of exposed organisms. Panels (A) and (B) are NOM OH-SWCNT-exposed organisms. Panels (C) and (D) are NOM PEG-SWCNT-exposed organisms. Panels (E) and (F) are NOM PABS-SWCNT-exposed organisms. Panel (G) is NOM SiO₂-SWCNT-exposed organism. Panels (H) and (I) are FBS OH-SWCNT-exposed organisms. Suspected SWCNTs in the gut are outlined with rectangles and suspected material associated with the microvilli and absorbed in the lumen are outlined with squares.

SWCNTs absorption had occurred (Figures 4 and 5), it became clear with further analysis (HRTEM and SAD) that these structures were in fact staining artifacts or consisted of other, unidentified organic structures which lacked the characteristic traits of SWCNTs. We were unable to find SWCNTs in the tissues of any of the examined specimens, but were able to locate them in the gut tract for the PABS-SWCNTs using these techniques. This is not meant to definitively indicate that no absorption occurred, but rather that we were unable to detect as much using HRTEM imaging.

Given the lengths observed in the micrographs for the dried SWCNTs which ranged from 0.75 to 2 μm (Figure 1), we were surprised at the small size (≈ 10 nm in length) of some of the SWCNTs observed within the gut tract (Figure 5F). There may have been substantial nanotube damage during the sonication process, but we expected the nanotubes to be much larger. An alternate explanation is that many of the longer SWCNTs were removed during sample preparation. As determined by EELS, the thin sections used in the TEM imaging typically ranged from 100 to 200 nm in thickness. Given that the nanotubes observed in isolation were much longer than 200 nm (Figure 1), it is possible that many of the longer nanotubes were removed via a pullout mechanism during section preparation. In other words, nanotubes not directly aligned in the plane of the section may have been physically removed by the glass knife used to prepare the samples. However, we did not consistently observe large numbers of tears in the thin sections that would likely have been present if a large number of embedded nanotubes had been removed. In addition, the longest nanotubes are expected to be least likely to enter into daphnia tissues, so the sectioning approach is unlikely to have impacted our ultimate conclusions.

Another pitfall of the sample preparation was that the staining process created artifacts that were initially thought to be absorbed SWCNTs. The lead citrate counter stain may precipitate in the presence of CO₂, creating electron dense areas within samples, which, at low-magnification, may be incorrectly identified as CNTs. During the staining process, steps were taken to ensure that the lead citrate stain did not precipitate. The staining was performed in a covered container on a bed of NaOH beads, which are intended to absorb the CO₂, and the stain is filtered prior to use. However, when working at such a small scale it is difficult to prevent small amounts of precipitation in the stain. Figure S1 is an example of the potentially misleading artifacts resulting from the staining process. Figure S1A is an image of the FBS OH-SWCNT-exposed organism that was *not* stained compared to the same organism in stained sections in Figure 4H and I. Figure S1B is an image of a control organism where staining was used in the absence of SWCNTs. In comparing these images it becomes clear how the staining procedure can produce false positives during imaging due to the presence of precipitates in the specimen.

Conclusions

A variety of surface functionalized SWCNTs were tested to determine potential for uptake from the gut tract in *D. magna*. Results support the conclusion that SWCNTs did not move out of the gut tract and into the organism at concentrations detectable using the characterization techniques employed. Initial, low-magnification TEM images were very suggestive of carbon nanotube absorption into tissues. However, upon closer inspection, we were unable to confirm that these images actually contained nanotubes. While TEM seems the most logical technique to identify carbon nanotubes because of their size, we have shown that sample preparation may cause false positives that result in inaccurate conclusions such that care must be taken

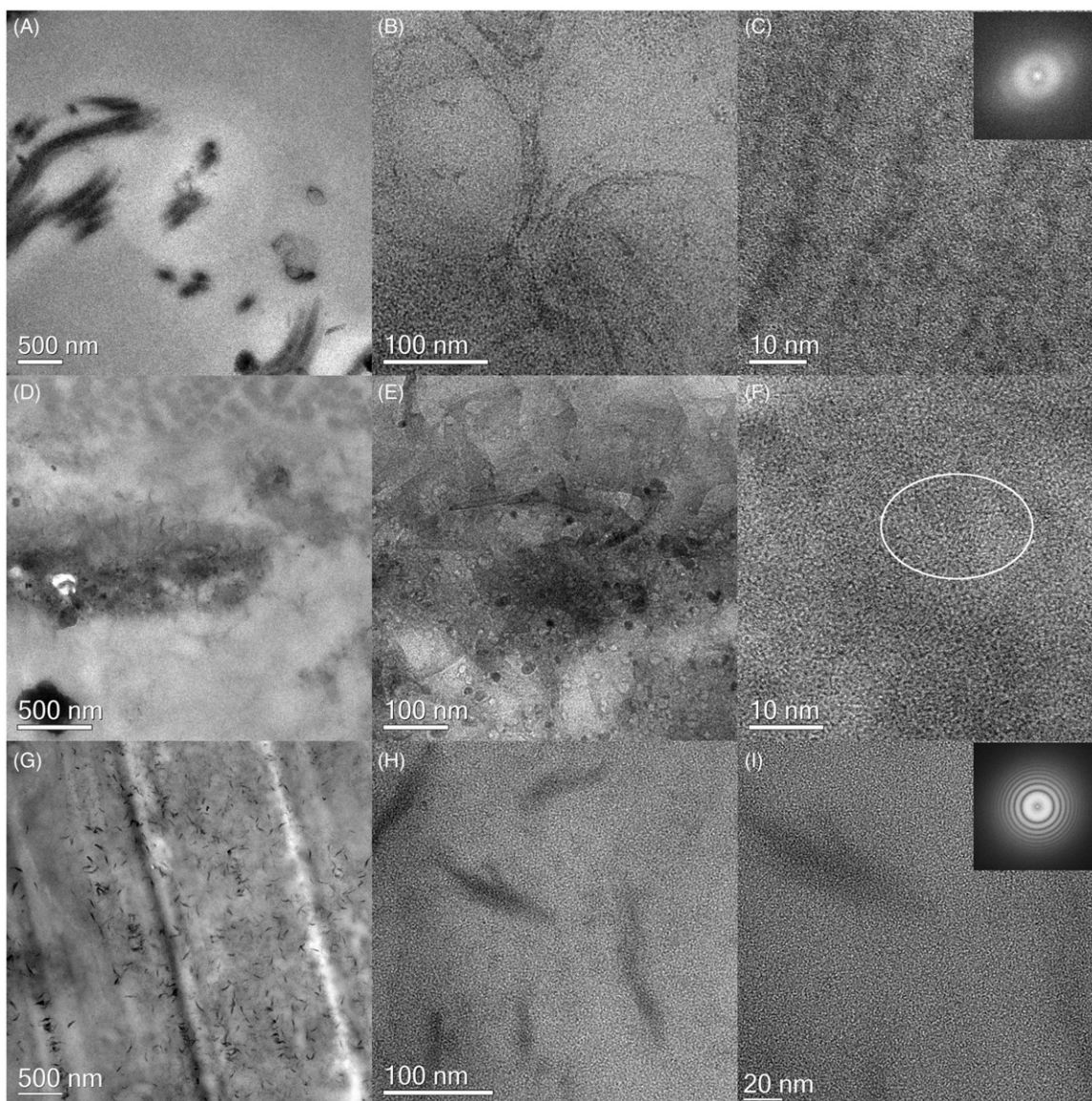


Figure 5. HRTEM images of suspected SWCNTs found within the gut tract of exposed *D. magna*. Panels (A), (B) and (C) are FBS OH-SWCNT exposed organism HRTEM images of tubular structures found within the gut tract and panel (C) is HRTEM image with SAD diffraction pattern (inset) confirming the absence of SWCNTs. Panels (D), (E) and (F) are micrographs of NOM PBS-SWCNTs imaged in exposed *D. magna* sections ranging from 100 nm (D) to 10 nm (F). A bundle of SWCNTs within the gut can be seen in circled region of panel (F). Panel (G) is a TEM image of tubular structures, and panels (H) and (I) are high-resolution images of those structures. The inset on panel (I) shows the diffractogram (FFT) that confirms the absence of crystalline material.

during image interpretation. Previous studies that have shown similar dark material in their sections may have in fact identified unknown organic matter or artifacts from the staining preparation that is standard protocol for producing quality TEM images. We have shown that it is not only necessary to use TEM but also additional analytical techniques, such as HR-TEM or SAD, to confirm the presence of embedded carbon nanotubes, especially in the case where a low concentration is expected. As the field of nanotoxicology continues to advance, it is imperative that we use the best and most advanced techniques to detect nanomaterials in biological matrices. Moreover, researchers are strongly encouraged to confirm the identity of particles that appear to be absorbed into organism tissues using complimentary technique to limit reports of false positive results. However, this manuscript also details many limitations and challenges of using TEM and its associated technique in order to determine SWCNTs uptake into organisms. TEM is not designed to be a survey technique so attempting to find an individual SWCNT in large areas of tissue

may be unfeasible especially given that beam damage will occur to resins with prolonged exposure to the high-energy electron beam. Additional analytical research is critical to determine the detection limit of analytical TEM for SWCNTs and other NPs in tissues, and complimentary validated standard methods for detection and quantification of SWCNTs in tissues are needed.

A potential future step for these investigations would be to embed SWCNTs in resin, in the absence of other biological material, in order to probe the detection limits of the various techniques and to develop best practices for their identification. For example, EELS has been commonly employed to characterize SWCNTs lying on a thin, amorphous support film. However, our results suggest that this technique, while useful for analyzing previously identified structures, cannot readily be used to survey large areas of tissue in an effort to locate individual SWCNTs, which may or may not be present. It seems more likely that this technique could be used to confirm the identity of SWCNTs in cross sections possessing large quantities of SWCNTs, as

described by Porter et al. (2007). However, additional research is needed to evaluate the sensitivity of this technique for SWCNTs embedded in various types of resins at low concentrations. Other emerging techniques such as NIRF microscopy are also promising alternatives for investigating the biodistribution of SWCNTs in organisms (Parks et al., 2013; Schierz et al., 2012). While a list of techniques that have been used to assess uptake and distribution of SWCNTs in ecological organisms has been recently provided (Petersen et al., 2011), several additional novel techniques have also been published for SWCNT quantification in environmental matrices (Doudrick et al., 2012; Parks et al., 2013; Plata et al., 2012; Schierz et al., 2012). While NIRF microscopy, for example, has been used to assess accumulation and distribution of SWCNTs spiked in food that was ingested by larvae of *Drosophila melanogaster*, limitations of this technique include the use of uncommon equipment and that it can only identify individually dispersed semiconducting SWCNTs (Doudrick et al., 2012; Petersen et al., 2011).

Declaration of interest

This work was funded by the U.S. Environmental Protection Agency's STAR program grant numbers R833886 and R834092.

Certain commercial equipment or materials are identified in this article in order to specify adequately the experimental procedure. Such identification does neither imply recommendation or endorsement by the National Institute of Standards and Technology, nor does it imply that the materials or equipment identified are necessarily the best available for the purpose.

References

- Cedervall T, Lynch I, Lindman S, Berggard T, Thulin E, Nilsson H, et al. 2007. Understanding the nanoparticle-protein corona using methods to quantify exchange rates and affinities of proteins for nanoparticles. *Proc Natl Acad Sci USA* 104:2050–5.
- Chappell MA, George AJ, Dontsova KM, Porter BE, Price CL, Zhou P, et al. 2009. Surfactive stabilization of multi-walled carbon nanotube dispersions with dissolved humic substances. *Environ Pollut* 157: 1081–7.
- Cheng WW, Lin ZQ, Wei BF, Zeng Q, Han B, Wei CX, et al. 2011. Single-walled carbon nanotube induction of rat aortic endothelial cell apoptosis: reactive oxygen species are involved in the mitochondrial pathway. *Int J Biochem Cell B* 43:564–72.
- Davoren M, Herzog E, Casey A, Cottineau B, Chambers G, Byrne HJ, Lyng FM. 2007. *In vitro* toxicity evaluation of single walled carbon nanotubes on human A549 lung cells. *Toxicol In Vitro* 21:438–48.
- Di Giorgio ML, Di Bucchianico S, Ragnelli AM, Aimola P, Santucci S, Poma A. 2011. Effects of single and multi walled carbon nanotubes on macrophages: cyto and genotoxicity and electron microscopy. *Mutat Res* 722:20–31.
- Doudrick K, Herckes P, Westerhoff P. 2012. Detection of carbon nanotubes in environmental matrices using programmed thermal analysis. *Environ Sci Technol* 46:12246–53.
- Edgington AJ, Roberts AP, Taylor LM, Alloy MM, Reppert J, Rao AM, et al. 2010. The influence of natural organic matter on the toxicity of multiwalled carbon nanotubes. *Environ Toxicol Chem* 29:2511–18.
- Egerton RF. 2009. Electron energy-loss spectroscopy in the TEM. *Rep Prog Phys* 72:016502. doi: 10.1088/0034-4885/72/1/016502.
- Ferguson PL, Chandler GT, Templeton RC, Demarco A, Scrivens WA, Englehart BA. 2008. Influence of sediment-amendment with single-walled carbon nanotubes and diesel soot on bioaccumulation of hydrophobic organic contaminants by benthic invertebrates. *Environ Sci Technol* 42:3879–85.
- Fraser TWK, Reinardy HC, Shaw BJ, Henry TB, Handy RD. 2011. Dietary toxicity of single walled carbon nanotubes and fullerenes (C₆₀) in rainbow trout (*Oncorhynchus mykiss*). *Nanotoxicology* 5:98–108.
- Galloway T, Lewis C, Dolciotti I, Johnston BD, Moger J, Regoli F. 2010. Sublethal toxicity of nano-titanium dioxide and carbon nanotubes in a sediment dwelling marine polychaete. *Environ Pollut* 158:1748–55.
- Gottschalk F, Sonderer T, Scholz RW, Nowack B. 2009. Modeled environmental concentrations of engineered nanomaterials (TiO₂, ZnO, CNT, Fullerenes) for different regions. *Environ Sci Technol* 43: 9216–22.
- Hyung H, Kim J. 2008. Natural organic matter (NOM) adsorption to multi-walled carbon nanotubes: effect of NOM characteristics and water quality parameters. *Environ Sci Technol* 42:4416–21.
- Hyung H, Fortner JD, Hughes JB, Kim J. 2007. Natural organic matter stabilizes carbon nanotubes in the aqueous phase. *Environ Sci Technol* 41:179–84.
- Iijima S. 1991. Helical microtubules of graphitic carbon. *Nature* 354: 56–8.
- Inoue KI, Yanagisawa R, Koike E, Nishikawa M, Takano H. 2010. Repeated pulmonary exposure to single-walled carbon nanotubes exacerbates allergic inflammation of the airway: possible role of oxidative stress. *Free Radic Biol* 48:924–34.
- Lam CW, James JT, McCluskey R, Hunter RL. 2004. Pulmonary toxicity of single-wall carbon nanotubes in mice 7 and 90 days after intratracheal instillation. *Toxicol Sci* 77:126–34.
- Lewis P, Klemm D, Lazorchak J, Norber-King T, Peltiet W, Heber M. 1994. Short-term Methods for Estimating the Chronic Toxicity of Effluents and Receiving Waters to Freshwater and Marine Organisms. EPA 600/4-91/002. Cincinnati, OH: U.S. Environmental Protection Agency.
- Lu C, Su F. 2007. Adsorption of natural organic matter by carbon nanotubes. *Sep Purif Technol* 58:113–21.
- Lundqvist M, Stigler J, Elia G, Lynch I, Cedervall T, Dawson KA. 2008. Nanoparticle size and surface properties determine the protein corona with possible implications for biological impacts. *Proc Natl Acad Sci USA* 105:14265–70.
- Maynard A, Aitken R, Colvin V, Donaldson K, Oberdorster G, Philbert M, et al. 2006. Safe handling of nanotechnology. *Nature* 444:267–9.
- Mouchet F, Landois P, Sarremejean E, Bernard G, Puech P, Pinelli E, et al. 2008. Characterization and *in vivo* ecotoxicity evaluation of double-wall carbon nanotubes in larvae of the amphibian *Xenopus laevis*. *Aquat Toxicol* 87:127–37.
- Mouchet F, Landois P, Puech P, Pinelli E, Flahaut E, Gauthier L. 2010. Carbon nanotube ecotoxicity in amphibians: assessment of multiwalled carbon nanotubes and comparison with double-walled carbon nanotubes. *Nanomedicine* 5:963–74.
- Niyogi S, Hamon MA, Hu H, Zhao B, Bhowmik P, Sen R, et al. 2002. Chemistry of single-walled carbon nanotubes. *Acc Chem Res* 35: 1105–13.
- Parks NA, Portis LM, Schierz PA, Washbur KM, Perron MM, Burgess RM, et al. 2013. Bioaccumulation and toxicity of single-walled carbon nanotubes to benthic organisms at the base of the marine food chain. *Environ Toxicol Chem* 32:1270–7.
- Petersen EJ, Huang QG, Weber Jr WJ. 2008a. Bioaccumulation of radiolabeled carbon nanotubes by *Eisenia foetida*. *Environ Sci Technol* 42: 3090–5.
- Petersen EJ, Huang QG, Weber Jr WJ. 2008b. Ecological uptake and depuration of carbon nanotubes by *Lumbricus variegatus*. *Environ Health Perspect* 116:496–500.
- Petersen EJ, Pinto RA, Landrum PF, Weber Jr WJ. 2009. Influence of carbon nanotubes on pyrene bioaccumulation from contaminated soils by earthworms. *Environ Sci Technol* 43:4181–7.
- Petersen EJ, Huang QG, Weber Jr WJ. 2010. Relevance of octanol-water distribution measurements to the potential ecological uptake of multi-walled carbon nanotubes. *Environ Toxicol Chem* 29:1106–12.
- Petersen EJ, Zhang LW, Mattison NT, O'Carroll DM, Whelton AJ, Uddin N, et al. 2011. Potential release pathways, environmental fate, and ecological risks of carbon nanotubes. *Environ Sci Technol* 45:9837–56.
- Plata DL, Reddy CM, Gschwend PM. 2012. Thermogravimetry-mass spectrometry for carbon nanotube detection in complex mixtures. *Environ Sci Technol* 46:12254–61.
- Porter AE, Gass M, Muller K, Skepper JN, Midgley PA, Welland M. 2007. Direct imaging of single-walled carbon nanotubes in cells. *Nat Nanotech* 2:713–17.
- Reed BW, Sarikaya M. 2002. TEM/EELS analysis of heat-treated carbon nanotubes: experimental techniques. *J Electron Microsc* 51:S97–105.
- Roberts AP, Mount AS, Seda B, Souther J, Qiao R, Lin S, et al. 2007. *In vivo* biomodification of lipid-coated carbon nanotubes by *Daphnia magna*. *Environ Sci Technol* 41:3025–9.
- Schierz A, Parks AN, Washburn KM, Chandler GT, Ferguson PL. 2012. Characterization and quantitative analysis of single-walled carbon nanotubes in the aquatic environment using near-infrared fluorescence spectroscopy. *Environ Sci Technol* 46:12262–71.

- Smith CJ, Shaw BJ, Handy RD. 2007. Toxicity of single walled carbon nanotubes to rainbow trout, (*Oncorhynchus mykiss*): respiratory toxicity, organ pathologies, and other physiological effects. *Aquat Toxicol* 82:94–109.
- Taurozzi JS, Hackley VA, Wiesner MR. 2010. Ultrasonic dispersion of nanoparticles for environmental, health, and safety assessment – issues and recommendations. *Nanotoxicology* 5:711–29.
- Templeton RC, Ferguson PL, Washburn KM, Scribens WA, Chandler GT. 2006. Life-cycle effects of single-walled carbon nanotubes (SWNTs) on an estuarine meiobenthic copepod. *Environ Sci Technol* 40:7387–93.
- U.S. Environmental Protection Agency. 1993. Methods for Measuring the Acute Toxicity of Effluents and Receiving Waters to Freshwater and Marine Organisms. EPA/600/4-90/027F. Cincinnati, OH: U.S. Environmental Protection Agency.
- Wang J, Sun P, Bao Y, Liu J, An L. 2011. Cytotoxicity of single-walled carbon nanotubes on PC12 cells. *Toxicol In Vitro* 25: 242–50.
- Zhang L, Petersen EJ, Huang Q. 2011. Phase distribution of ¹⁴C-labeled multi-walled carbon nanotubes in aqueous systems containing model solids: peat. *Environ Sci Technol* 44:1356–62.

Supplementary material available online

Supplementary Figure 1